

A Characteristic Nonoverlapping Domain Decomposition Method for Multidimensional Convection-Diffusion Equations

Hong Wang,¹ Jianguo Liu,² Magne S. Espedal,³ Richard E. Ewing²

¹*Department of Mathematics, University of South Carolina, Columbia, South Carolina 29208*

²*Institute for Scientific Computation, Texas A&M University, College Station, Texas 77843-3404*

³*Department of Mathematics, University of Bergen, Johs. Brunsgt. 12, N-5007, Bergen, Norway*

Received 18 November 2002; accepted 15 March 2004

Published online 18 May 2004 in Wiley InterScience (www.interscience.wiley.com).

DOI 10.1002/num.20025

We develop a quasi-two-level, coarse-mesh-free characteristic nonoverlapping domain decomposition method for unsteady-state convection-diffusion partial differential equations in multidimensional spaces. The development of the domain decomposition method is carried out by utilizing an additive Schwarz domain decomposition preconditioner, by using an Eulerian-Lagrangian method for convection-diffusion equations and by delicately choosing appropriate interface conditions that fully respect and utilize the hyperbolic nature of the governing equations. Numerical experiments are presented to illustrate the method. © 2004 Wiley Periodicals, Inc. *Numer Methods Partial Differential Eq* 21: 89–103, 2005

Keywords: additive Schwarz preconditioner; convection-diffusion equation; characteristic method; Eulerian-Lagrangian method; nonoverlapping domain decomposition method

I. INTRODUCTION

Unsteady-state (time-dependent) convection-diffusion partial differential equations (PDEs) arise in petroleum reservoir simulation, subsurface contaminant remediation, and many other applications. These problems admit solutions with moving sharp fronts and complicated structures, which present serious numerical difficulties. Furthermore, an identifying feature of these applications is the presence of extremely large-scale fluid flows coupled with transient transport of physical quantities such as pollutants and temperature. Therefore, an extremely refined global

Correspondence to: Jianguo Liu, Institute for Scientific Computation, Texas A&M University, College Station, TX 77843-3404 (e-mail: jliu@isc.tamu.edu)

© 2004 Wiley Periodicals, Inc.

mesh will result in excessive computational cost. Domain decomposition methods (DDMs) provide a feasible approach for handling these problems. Different physical, mathematical, or numerical models can be set up on different subdomains based on the properties and scales of the problems. Moreover, the subproblems in different subdomains can be solved in parallel, by using DDMs as an iterative solution procedure or as a preconditioner. Nevertheless, many DDMs that are well suited for elliptic or parabolic PDEs [1, 2] could have a less promising performance for convection-diffusion PDEs. The fundamental reason for this is that these methods do not necessarily respect the hyperbolic nature of convection-diffusion PDEs. Cai [3, 4] developed and analyzed multilevel additive and multiplicative Schwarz DDM preconditioners for non-self-adjoint parabolic PDEs. The Adaptive Dirichlet-Neumann and Adaptive Robin-Neumann nonoverlapping DDMs [5, 6] choose the interface matching conditions to be adapted to local flow direction in solving stationary convection-diffusion PDEs. Numerical damping effect is introduced in [7] via a streamline diffusion finite element method. Because the underlying methods are Eulerian type, these DDMs generate discrete algebraic systems with strongly nonsymmetric coefficient matrices at each time step. Hence, these methods tend to require extra computational effort and cost [8].

Eulerian-Lagrangian methods [9, 10] carry out temporal discretization along characteristics by combining the advective component with the accumulation term through characteristic tracking and treat the diffusion separately in an Eulerian manner. They symmetrize the governing equations and generate accurate numerical solutions even if large time steps are used. Hence, several overlapping characteristic DDMs [11] have been developed for convection-diffusion PDEs, which have demonstrated the strength of characteristic DDMs. However, few characteristics nonoverlapping DDMs can be found in the literature, partly due to the fact that many earlier characteristic methods have difficulties in treating general boundary conditions. In such applications as mathematical and numerical modeling of subsurface flow through porous media with physical or numerical interfaces, nonoverlapping DDMs are particularly preferred.

In this article we develop a quasi-two-level, coarse-mesh-free characteristic nonoverlapping DDM for time-dependent convection-diffusion PDEs in multiple space dimensions. The DDM is developed based upon an Eulerian-Lagrangian localized adjoint method (ELLAM), which solves time-dependent convection-diffusion PDEs with general boundary conditions in a conservative manner [12]. The development of the DDM is carried out by using an additive Schwarz DDM framework, by taking the full advantages of the Lagrangian nature of convection-diffusion PDEs (e.g., finite propagation speed of advective transport, virtually local information exchange), and by delicately choosing appropriate interface conditions that fully respect and utilize the hyperbolic nature of the governing equations.

The rest of this article is organized as follows. In section II we outline an underlying ELLAM formulation for convection-diffusion PDEs. In section III we develop a nonoverlapping coarse-mesh-free characteristic DDM. In section IV we present numerical experiments to show the strong potential of the method. Finally a summary is given in section V.

II. AN UNDERLYING EULERIAN-LAGRANGIAN FORMULATION

An excellent overview about the current state of research on ELLAM was given in [13]. In this section, we apply the ELLAM methodology to study the following unsteady-state linear convection-diffusion PDE

$$u_t + \nabla \cdot (\mathbf{v}u - \mathbf{D}\nabla u) = f(\mathbf{x}, t), \quad \mathbf{x} \in \Omega, \quad t \in [0, T], \quad (2.1)$$

and outline an ELLAM scheme for (2.1). Here Ω is a domain in \mathbb{R}^d with boundary $\Gamma := \partial\Omega$; $u(\mathbf{x}, t)$ is the unknown function; $\mathbf{v}(\mathbf{x}, t)$ is a velocity field; $\mathbf{D}(\mathbf{x}, t)$ is a diffusion-dispersion tensor; and $f(\mathbf{x}, t)$ is a source/sink term.

Let Γ^I , Γ^O , and Γ^N be the inflow, outflow, and noflow boundaries identified by

$$\Gamma^I := \{\mathbf{x} | \mathbf{x} \in \Gamma, \mathbf{v} \cdot \mathbf{n} < 0\}, \quad \Gamma^O := \{\mathbf{x} | \mathbf{x} \in \Gamma, \mathbf{v} \cdot \mathbf{n} > 0\}, \quad \Gamma^N := \{\mathbf{x} | \mathbf{x} \in \Gamma, \mathbf{v} \cdot \mathbf{n} = 0\}, \quad (2.2)$$

where $\mathbf{n}(\mathbf{x})$ is the outward unit normal vector. The ELLAM framework can treat any boundary conditions [12, 14]. But we restrict ourselves to the following boundary and initial conditions that are typical in applications:

$$\begin{aligned} u(\mathbf{x}, t) &= g^O(\mathbf{x}, t), & \mathbf{x} \in \Gamma^O, & \quad t \in [0, T], \\ (\mathbf{v}u - \mathbf{D}\nabla u)(\mathbf{x}, t) \cdot \mathbf{n} &= g^I(\mathbf{x}, t), & \mathbf{x} \in \Gamma^I, & \quad t \in [0, T], \\ -\mathbf{D}\nabla u(\mathbf{x}, t) \cdot \mathbf{n} &= 0, & \mathbf{x} \in \Gamma^N, & \quad t \in [0, T], \\ u(\mathbf{x}, 0) &= u_0(\mathbf{x}), & \mathbf{x} \in \Omega. & \end{aligned} \quad (2.3)$$

Let $0 = t_0 < t_1 < \dots < t_{n-1} < t_n < \dots < t_N = T$ be a partition of $[0, T]$ with $\Delta t_n := t_n - t_{n-1}$. We multiply Equation (2.1) by test functions $w(\mathbf{x}, t)$ that vanish outside the space-time strip $\Omega \times (t_{n-1}, t_n]$ and are discontinuous in time at time t_{n-1} . Then integration by parts leads us to the following weak form:

$$\begin{aligned} \int_{\Omega} u(\mathbf{x}, t_n) w(\mathbf{x}, t_n) d\mathbf{x} + \int_{t_{n-1}}^{t_n} \int_{\Omega} (\mathbf{D}\nabla u) \cdot \nabla w d\mathbf{x} dt + \int_{t_{n-1}}^{t_n} \int_{\partial\Omega} (\mathbf{v}u - \mathbf{D}\nabla u) \cdot \mathbf{n} w dS \\ - \int_{t_{n-1}}^{t_n} \int_{\Omega} u(w_t + \mathbf{v} \cdot \nabla w) d\mathbf{x} dt = \int_{\Omega} u(\mathbf{x}, t_{n-1}) w(\mathbf{x}, t_{n-1}^+) d\mathbf{x} + \int_{t_{n-1}}^{t_n} \int_{\Omega} (fw)(\mathbf{x}, t) d\mathbf{x} dt, \end{aligned} \quad (2.4)$$

where dS is the differential element on $\partial\Omega$ and $w(\mathbf{x}, t_{n-1}^+) := \lim_{t \rightarrow t_{n-1}^+} w(\mathbf{x}, t)$ takes into account the fact that $w(\mathbf{x}, t)$ is discontinuous in time at time t_{n-1} .

The ELLAM formalism takes advantage of the hyperbolic nature of convection-diffusion PDEs to require the test functions to satisfy the adjoint equation:

$$w_t + \mathbf{v} \cdot \nabla w = 0. \quad (2.5)$$

This cancels the last term on the left side of the weak form and implies that test functions are constants along the characteristics defined by the initial value problem to ordinary differential equations:

$$\begin{cases} \frac{dy}{ds} = \mathbf{v}(\mathbf{y}, s) \\ \mathbf{y}(s; \mathbf{x}, t)|_{s=t} = \mathbf{x} \end{cases} \quad (2.6)$$

For convenience, we denote $\Gamma_n^I := \Gamma^I \times [t_{n-1}, t_n]$, $\Gamma_n^O := \Gamma^O \times [t_{n-1}, t_n]$, and $\Gamma_n^N := \Gamma^N \times [t_{n-1}, t_n]$. For any $\mathbf{x} \in \Omega$, if (\mathbf{x}, t_n) backtracks along characteristic to $(\mathbf{x}_*, t_*) \in \Gamma_n^I$ or Ω

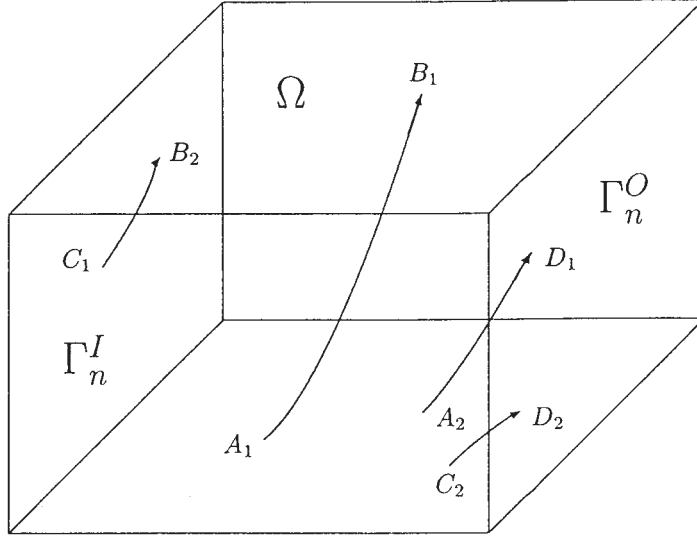


FIG. 1. Characteristics and flows.

at time t_{n-1} , we define $\Delta t^I(\mathbf{x}, t_n) := t_n - t_*$ or $t_n - t_{n-1}$, respectively. Similarly, for any $(\mathbf{y}, t) \in \Gamma_n^O$, if it backtracks to $(\mathbf{y}_*, t_*) \in \Gamma_n^I$ or Ω at time t_{n-1} , we define $\Delta t^O(\mathbf{y}, t) := t - t_*$ or $t_n - t_{n-1}$, respectively.

Figure 1 provides a graphic illustration of various possibilities in the characteristic tracking, under the assumption that the spatial domain Ω is a two-dimensional rectangular domain and that the left and front faces of the space-time domain $\Omega \times [t_{n-1}, t_n]$ are inflow boundary and the right and back faces are outflow boundary. In Fig. 1, A_1 and A_2 are in Ω at time t_{n-1} , while B_1 and B_2 are in Ω at time t_n . C_1 and C_2 are on the inflow boundary Γ_n^I , while D_1 and D_2 are on the outflow boundary Γ_n^O .

By enforcing backward Euler quadrature on Ω at time t_n and Γ_n^O , we obtain

$$\int_{t_{n-1}}^{t_n} \int_{\Omega} f(\mathbf{x}, t) w(\mathbf{x}, t) d\mathbf{x} dt = \int_{\Omega} \Delta t^I(\mathbf{x}, t_n) f(\mathbf{x}, t_n) w(\mathbf{x}, t_n) d\mathbf{x} + \int_{\Gamma_n^O} \Delta t^O(\mathbf{y}, t) f(\mathbf{y}, t) w(\mathbf{y}, t) (\mathbf{v} \cdot \mathbf{n}) dS + E(f, w).$$

Similarly, the diffusion term can be evaluated as

$$\int_{t_{n-1}}^{t_n} \int_{\Omega} ((\mathbf{D}\nabla u) \cdot \nabla w)(\mathbf{x}, t) d\mathbf{x} dt = \int_{\Omega} \Delta t^I(\mathbf{x}, t_n) ((\mathbf{D}\nabla u) \cdot \nabla w)(\mathbf{x}, t_n) d\mathbf{x} + \int_{\Gamma_n^O} \Delta t^O(\mathbf{y}, t) ((\mathbf{D}\nabla u) \cdot \nabla w)(\mathbf{y}, t) (\mathbf{v} \cdot \mathbf{n}) dS + E(D, u, w).$$

The above two formulas rely on backward Euler quadrature to approximate the corresponding integrals in the weak form (2.4). It should be pointed out that higher order numerical quadratures have also been used to establish ELLAM formulation [15, 16].

Dropping the error terms in the source and diffusion terms and breaking up the boundary term, we obtain the following weak formulation: Find $u(\mathbf{x}, t) \in H^1(\Omega \times (t_{n-1}, t_n])$ such that for any $w(\mathbf{x}, t) \in H^1(\Omega \times (t_{n-1}, t_n])$ satisfying the adjoint equation (2.5), the following holds

$$\begin{aligned}
 & \int_{\Omega} u(\mathbf{x}, t_n)w(\mathbf{x}, t_n)d\mathbf{x} + \int_{\Omega} \Delta t^l(\mathbf{x}, t_n)(\mathbf{D}\nabla u \cdot \nabla w)(\mathbf{x}, t_n)d\mathbf{x} + \int_{\Gamma_n^o} \Delta t^o(\mathbf{y}, t)(\mathbf{D}\nabla u) \cdot \nabla w(\mathbf{y}, t)(\mathbf{v} \cdot \mathbf{n})dS \\
 & + \int_{\Gamma_n^o} (\mathbf{v}u - \mathbf{D}\nabla u) \cdot \mathbf{n}w(\mathbf{y}, t)dS + \int_{\Gamma_n^i} (\mathbf{v}u - \mathbf{D}\nabla u) \cdot \mathbf{n}w(\mathbf{y}, t)dS = \int_{\Omega} u(\mathbf{x}, t_{n-1})w(\mathbf{x}, t_{n-1}^+)d\mathbf{x} \\
 & + \int_{\Omega} \Delta t^l(\mathbf{x}, t_n)f(\mathbf{x}, t_n)w(\mathbf{x}, t_n)d\mathbf{x} + \int_{\Gamma_n^o} \Delta t^o(\mathbf{y}, t)f(\mathbf{y}, t)w(\mathbf{y}, t)(\mathbf{v} \cdot \mathbf{n})dS. \tag{2.7}
 \end{aligned}$$

III. A CHARACTERISTIC NONOVERLAPPING DOMAIN DECOMPOSITION METHOD

The ELLAM formulation (2.7) yields a discrete algebraic system with a banded, symmetric, and positive-definite (SPD) coefficient matrix [8, 12, 14]. Therefore, the ELLAM scheme can be solved by conjugate gradient (CG) types of methods. It can also be used in the construction of an additive Schwarz domain decomposition preconditioner to expedite the convergence of the PCG method.

A. An Additive Schwarz Preconditioner

Let \mathbf{A} be the coefficient matrix of the ELLAM formulation (2.7) and \mathbf{B} be an SPD preconditioner of \mathbf{A} . Let \mathbf{u} be the resulting solution vector with its entries being the nodal values of the ELLAM solution, and \mathbf{u}_k be the k th iterative solution. Then the convergence rate of a preconditioned conjugate gradient (PCG) method is

$$\|\mathbf{u}_k - \mathbf{u}\|_{\mathbf{A}} \leq 2 \left(\frac{\sqrt{\kappa(\mathbf{B}\mathbf{A})} - 1}{\sqrt{\kappa(\mathbf{B}\mathbf{A})} + 1} \right)^k \|\mathbf{u}_0 - \mathbf{u}\|_{\mathbf{A}}, \tag{3.1}$$

where $\|\cdot\|_{\mathbf{A}} := \sqrt{(\mathbf{A}\cdot, \cdot)}$ is the discrete energy norm and $\kappa(\mathbf{A}) := \lambda_{\max}(\mathbf{A})/\lambda_{\min}(\mathbf{A})$ is the condition number of \mathbf{A} .

A great deal of effort has been cast into constructing good preconditioners that are computationally inexpensive and reduce the condition number $\kappa(\mathbf{B}\mathbf{A})$ significantly. The additive Schwarz DDM proves to be a very effective preconditioner. Let V be an n -dimensional vector space with V' being its dual space, and V_j ($j = 1, \dots, J$) be auxiliary vector spaces. Let $\mathbf{A} : V \rightarrow V'$ and $\mathbf{A}_j : V_j \rightarrow V_j'$ be SPD operators, and $\mathbf{I}_j : V_j \rightarrow V$ be linear operators connecting the auxiliary spaces V_j to the space V . If the following space decomposition holds

$$V = \sum_{j=1}^J \mathbf{I}_j(V_j), \tag{3.2}$$

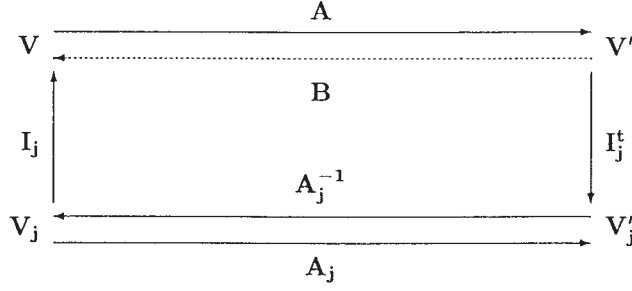


FIG. 2. Abstract additive Schwarz preconditioner.

then an abstract additive Schwarz preconditioner $\mathbf{B} : V' \rightarrow V$ for \mathbf{A} is constructed as follows [1, 17]:

$$\mathbf{B} := \sum_{j=0}^J \mathbf{I}_j \mathbf{A}_j^{-1} \mathbf{I}_j^t, \tag{3.3}$$

where \mathbf{A}_j^{-1} is the inverse operator of \mathbf{A}_j and \mathbf{I}_j^t is the transpose of \mathbf{I}_j (see Fig. 2).

B. Artificial Boundary Conditions and Interface Matching Conditions

To develop a characteristic nonoverlapping DDM, we use the ELLAM formulation (2.7) as an underlying numerical scheme to solve the governing convection-diffusion PDE (2.1) over the global domain Ω . We also use a modified ELLAM formulation as a subdomain solver on each subdomain Ω_j in an abstract two-level additive Schwarz preconditioner (3.3). To do so, we need to specify artificial inflow or outflow boundary conditions on the internal boundary $\partial\Omega_j \setminus \Gamma$ of the subdomain Ω_j . We also need to propose appropriate interface matching conditions for adjacent subdomains. It is known that boundary conditions for convection-diffusion PDEs are not symmetric with respect to the inflow and outflow boundaries. The numerical solutions to convection-diffusion equations are very sensitive to flow directions and the types of boundary conditions specified at inflow or outflow boundaries [14, 18]. Therefore, the artificial inflow and outflow boundary conditions at the boundaries of each subdomain must be chosen carefully. Notice that physically the total flux must be continuous across an interface. The unknown function should be continuous (or at least the left- and right-limits of the function should satisfy certain condition as in the case of multiphase flows) across an interface. Thus, we choose Robin and Dirichlet conditions as interface matching conditions (see Fig. 3).

C. A Modified ELLAM Scheme on Subdomains

For each subdomain Ω_j , we identify its inflow boundary $\partial\Omega_j^I$, outflow boundary $\partial\Omega_j^O$, and noflow boundary $\partial\Omega_j^N$ by

$$\partial\Omega_j^I := \{\mathbf{x} | \mathbf{x} \in \partial\Omega_j, \mathbf{v} \cdot \mathbf{n} < 0\}, \partial\Omega_j^O := \{\mathbf{x} | \mathbf{x} \in \partial\Omega_j, \mathbf{v} \cdot \mathbf{n} > 0\}, \partial\Omega_j^N := \{\mathbf{x} | \mathbf{x} \in \partial\Omega_j, \mathbf{v} \cdot \mathbf{n} = 0\}. \tag{3.4}$$

Let $S_h := S_h(\Omega_j)$ be the space of continuous piecewise linear polynomials on Ω_j associated with the partition given by the restriction of the partition \mathcal{T}_h on Ω_j . We define the finite element trial space $S_h^{tr}(\Omega_j)$ to be the restriction of $S_h(\Omega)$ on Ω_j . For test functions, we add the test

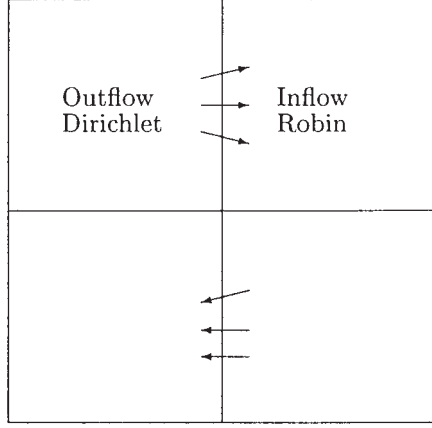


FIG. 3. Internal boundary conditions.

functions associated with the nodes on the outflow boundary $\partial\Omega_j^O$ to the test functions at their neighboring nodes on the same element [14]. The corresponding test space is denoted by $S_h^{out}(\Omega_j)$. A modified ELLAM scheme based on the ELLAM formulation (2.7) on Ω_j can be formulated as follows: Seek $U \in S_h^{trI}(\Omega_j)$ with $U = g^O$ on $\partial\Omega_j$ such that

$$\begin{aligned} \int_{\Omega_j} U(\mathbf{x}, t_n)w(\mathbf{x}, t_n)d\mathbf{x} + \int_{\Omega_j} \Delta t_j^I(\mathbf{x}, t_n)(\mathbf{D}\nabla U \cdot \nabla w)(\mathbf{x}, t_n)d\mathbf{x} &= \int_{\Omega_j} U(\mathbf{x}, t_{n-1})w(\mathbf{x}, t_{n-1}^+)d\mathbf{x} \\ + \int_{\Omega_j} \Delta t_j^I(\mathbf{x}, t_n)f(\mathbf{x}, t_n)w(\mathbf{x}, t_n)d\mathbf{x} - \int_{t_{n-1}}^{t_n} \int_{\partial\Omega_j^I} g^I(\mathbf{y}, t)w(\mathbf{y}, t)dS. \end{aligned} \quad (3.5)$$

On $\partial\Omega_j^I \cap \Gamma^I$, we use the prescribed Robin data $g^I(\mathbf{x}, t)$ given in (2.3). Then $\Delta t_j^I(\mathbf{x}, t_n)$ in (3.5) is just $\Delta t^I(\mathbf{x}, t_n)$ defined in the ELLAM reference equation (2.7). On $\partial\Omega_j^I \setminus \Gamma^I$, we take

$$g^I(\mathbf{x}, t_n) := (\mathbf{v}u - \mathbf{D}\nabla u)(\mathbf{x}_*, t_{n-1}) \quad \text{with } \mathbf{x}_* := \mathbf{y}(t_{n-1}; \mathbf{x}, t_n) \quad (3.6)$$

and

$$\Delta t_j^I(\mathbf{x}, t_n) := \Delta t_n. \quad (3.7)$$

Similarly, on $\partial\Omega_j^O \cap \Gamma^O$, we use the prescribed Dirichlet data $g^O(\mathbf{x}, t)$ given in (2.3). On $\partial\Omega_j^O \setminus \Gamma^O$, we define an artificial outflow Dirichlet boundary data by

$$g^O(\mathbf{x}, t_n) := U(\mathbf{x}_*, t_{n-1}) \quad \text{with } \mathbf{x}_* := \mathbf{y}(t_{n-1}; \mathbf{x}, t_n). \quad (3.8)$$

In general, a blind specification of an artificial Dirichlet boundary data often introduces artificial boundary layers and causes numerical difficulties. Here, we fully utilize the hyperbolic nature

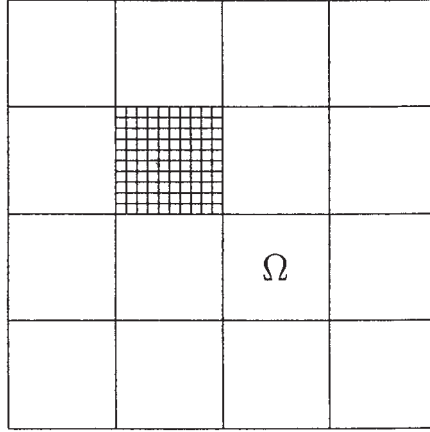


FIG. 4. Local versus global labeling of nodes.

of convection-diffusion PDEs to specify a Dirichlet condition based on characteristic tracking. The errors incurred are small, as pointed out in [14].

D. A Quasi-Two-Level Coarse-Mesh-Free Characteristic Nonoverlapping DDM

After artificial boundary conditions and interface matching conditions are specified as above, the ELLAM formulation (2.7) on the global domain Ω and (3.5) on subdomains Ω_j for $j = 1, \dots, J$ will produce SPD coefficient matrices. Let $V := \mathcal{S}_h(\Omega)$ and $V_j := \mathcal{S}_h(\Omega_j)$ for $j = 1, \dots, J$, then by construction

$$V = \mathbf{I}_1(V_1) + \dots + \mathbf{I}_J(V_J), \quad (3.9)$$

where \mathbf{I}_j is the mapping from the local nodal labeling on subdomain Ω_j to the global nodal labeling on the whole domain Ω as illustrated in Fig. 4, and \mathbf{I}_j^t is the corresponding reversal mapping. Thus, the current setting fits into the abstract additive Schwarz framework. Therefore, we can construct an additive Schwarz domain decomposition preconditioner according to (3.3).

The iterations in PCG involve multiplications of the matrices \mathbf{A} and \mathbf{B} with vectors. Because the coefficient matrix \mathbf{A} is sparse and SPD, the operation $\mathbf{A}\mathbf{v}$ needs computations on the order of number of unknowns and is straightforward. However, the operation $\mathbf{B}\mathbf{v}$ requires some extra work. Notice that

$$\mathbf{B}\mathbf{v} = \sum_{j=1}^J (\mathbf{I}_j \mathbf{A}_j^{-1} \mathbf{I}_j^t) \mathbf{v}. \quad (3.10)$$

The multiplication of \mathbf{I}_j^t or \mathbf{I}_j with a vector is just a *restriction* or *prolongation* of the vector. Let $\mathbf{w} := \mathbf{I}_j^t \mathbf{v}$ and $\mathbf{A}_j \mathbf{w} = \mathbf{v}$. In general, we do not compute or formulate \mathbf{A}_j^{-1} explicitly, because it is very expensive to compute and no longer a sparse matrix even though \mathbf{A}_j is. Any suitable *exact* or *inexact* solver can be used to implement the action of \mathbf{A}_j^{-1} by solving the local problem via a direct or iterative algorithm. For example, it can be a multigrid solver or a recursive use of the current DDM preconditioner.

The artificial boundary conditions (3.6) and (3.8) defined along the characteristics from the solution at the previous time step can be viewed as a coarse mesh solution, in the quasi-two-level, characteristic nonoverlapping DDM. In the context of convection-diffusion PDE (2.1), convection dominates fluid flow process. Hence, the propagation of information is virtually local. Consequently, the coarse mesh solution generated via the artificial boundary conditions across subdomain boundaries provides a fairly accurate approximation. The effect of diffusion is picked up via the ELLAM formulation in the DDM. Some of the authors previously derived optimal-order asymptotic error estimates for ELLAM schemes for linear convection-diffusion PDEs in multiple space dimensions [18, 19]. The theoretical estimates for two-level additive Schwarz DDMs can be found in [17] for elliptic PDEs, while estimates for DDMs for non self-adjoint parabolic PDEs can be found in [3, 4]. A theoretical error estimate for the characteristic nonoverlapping DDM developed in this article will be studied in subsequent articles.

IV. NUMERICAL EXPERIMENTS

In this section we carry out numerical experiments to investigate the performance of the characteristic nonoverlapping DDM developed in this article. In the numerical experiments, we use the standard CG algorithm as an inner iterative solver to solve the modified ELLAM scheme (3.5) on each subdomain Ω_j in the nonoverlapping additive Schwarz preconditioner (3.3). Then we use the PCG algorithm equipped with the nonoverlapping additive Schwarz preconditioner (3.3) as an outer iterative solver for the ELLAM scheme (2.7) imposed on the global domain Ω .

A. A Rotating Gaussian Pulse

In this subsection, we consider the transport of a rotating Gaussian pulse in a two-dimensional square domain. In the example run, the velocity field is given by $V_1(x, y) = -4y$, $V_2(x, y) = 4x$, and the diffusion tensor is taken as $\mathbf{D} = D\mathbf{I}$ with D being a positive constant. The source $f = 0$ and the initial condition is

$$u_0(x, y) = \exp\left(-\frac{(x - x_c)^2 + (y - y_c)^2}{2\sigma^2}\right), \quad (4.1)$$

where (x_c, y_c) and σ are the center and standard deviation, respectively. The analytical solution for this problem is given by

$$u(x, y, t) = \frac{2\sigma^2}{2\sigma^2 + 4Dt} \exp\left(-\frac{(x_* - x_c)^2 + (y_* - y_c)^2}{2\sigma^2 + 4Dt}\right), \quad (4.2)$$

where

$$\begin{cases} x_* = (\cos 4t)x + (\sin 4t)y, \\ y_* = -(\sin 4t)x + (\cos 4t)y. \end{cases} \quad (4.3)$$

Additional data are given as follows: $\Omega = [-0.5, 0.5] \times [-0.5, 0.5]$, $T = \pi/2$, $D = 0.0005$, $(x_c, y_c) = (-0.25, 0)$, $\sigma = 0.0447$, $\Delta t = \pi/32$, $h = 1/128$, and 10^{-6} as the tolerance for both

TABLE I. Results for rotating Gaussian pulse with $h = 1/128$.

	Exact solution	No decomposition	2×2 decomposition
U_{\max}	0.560, 095	0.561, 706, 477	0.561, 704, 0.28
U_{\min}	0.0	0.0	0.0
L^∞ error	N/A	0.002, 369, 060	0.002, 369, 007
L^2 error	N/A	0.000, 107, 382	0.000, 107, 385
L^1 error	N/A	0.000, 022, 735	0.000, 022, 749

the interior CG iterative solver on each subdomain and the outer PCG iterative solver on the global domain.

This problem provides an example of a transient two-dimensional homogeneous convection-diffusion PDE with a variable velocity field and a known analytical solution and can be viewed as an incompressible fluid flow through a two-dimensional homogeneous porous medium. Moreover, this problem switches from convection dominance in most of the domain to diffusion dominance in the region that is close to the origin. These types of problems often arise in many important applications and are more difficult to handle compared with purely convection- or diffusion-dominated problems. Consequently, this example has been used widely to test for numerical artifacts of different schemes, such as numerical stability, numerical dispersion, spurious undershoot or overshoot, deformation, and phase errors as well as other numerical effects arising in porous medium fluid flows [8, 14, 20].

Previous numerical experiments [8, 14, 15] revealed that some widely used numerical methods could suffer from one or a combination of the numerical artifacts mentioned above. These experiments also show that ELLAM schemes generate accurate numerical solutions that are free of these numerical artifacts, even if very large spatial grids and time steps are used. The objective of the numerical experiments in this section is to investigate whether the characteristic nonoverlapping DDM based on the ELLAM formulation (2.7) inherits the numerical advantages of the ELLAM schemes and is free of the numerical artifacts that are typical for numerical methods for transient convection-diffusion PDEs. To carefully study the performance of the characteristic nonoverlapping DDM, we present the error between the DDM solution and the analytical solution as well as the error between the ELLAM solution (without using DDM) and the analytical solution in L^1 , L^2 , and L^∞ norms in Table I. In addition, we measure the maximum and minimum of the DDM solution, the ELLAM solution, and the analytical solution in Table I to observe any possible undershoot or overshoot of the DDM solution. We present the surface and contour plots of the DDM solution and the analytical solution in Fig. 5. These experiments illustrate that the characteristic nonoverlapping DDM solution is comparable with the ELLAM solution without domain decomposition, while the ELLAM scheme has been shown to be very competitive with many widely used numerical methods for time-dependent convection-diffusion PDEs [8, 14, 15].

B. A Horizontal Flow

In this subsection, we carry out numerical experiments to observe the convergence behavior of the additive Schwarz DDM preconditioner. In the example run, the spatial domain $\Omega = [0, 1] \times [0, 1]$ and the time interval $[0, T] = [0, 0.7]$. The velocity field is given by $V_1(x, y) \equiv 1$ and $V_2(x, y) \equiv 0$. The diffusion-dispersion tensor is diagonal

$$\mathbf{D} = \begin{pmatrix} D_{11} & 0 \\ 0 & D_{22} \end{pmatrix},$$

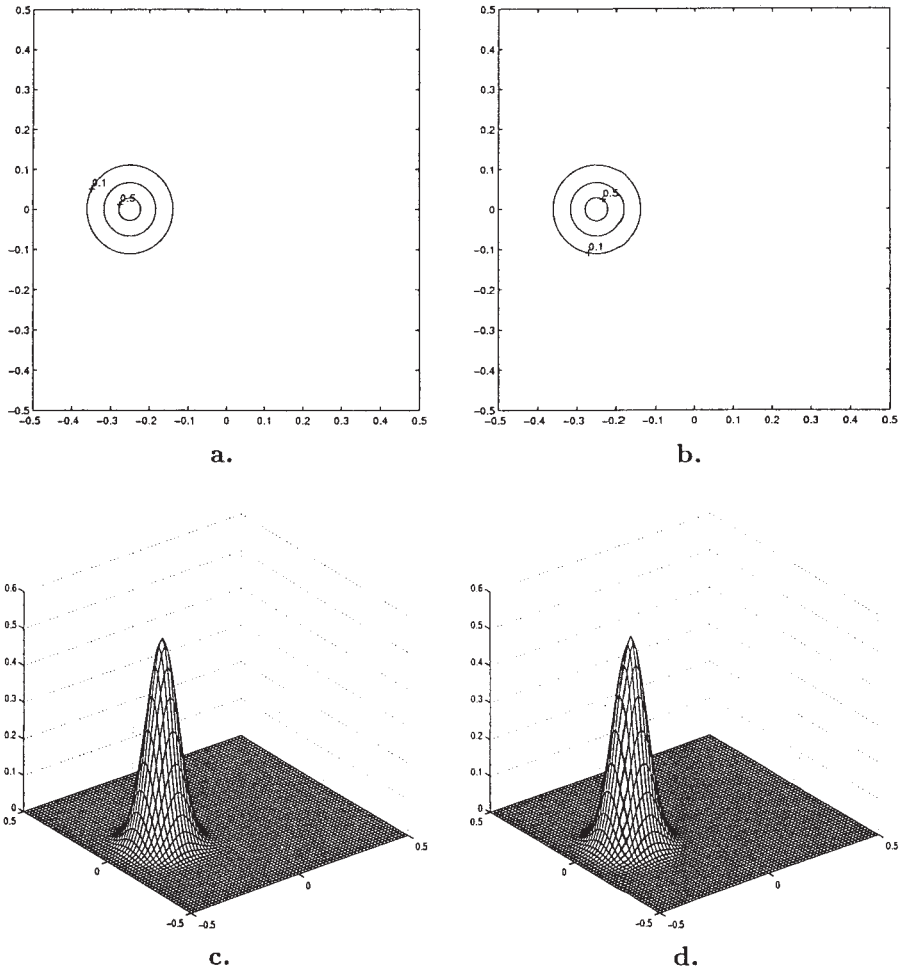


FIG. 5. Contour and surface plots of Gaussian pulse with $D = 0.0005$. (a) Exact solution; (b) $h = 1/128$, 2×2 subdomains; (c) exact solution; (d) $h = 1/128$, 2×2 subdomains.

with diagonal entries D_{11} and D_{22} being piecewise constants as shown in Fig. 6.

A discontinuous inflow Robin boundary data is specified on the left side of the domain

$$g(y) = \begin{cases} 1 & |y - \frac{1}{2}| \leq \frac{1}{32} \\ 0 & \text{otherwise} \end{cases} \quad (4.4)$$

and accordingly

$$g^I := (\mathbf{v}g - \mathbf{D}\nabla g) \cdot \mathbf{n}. \quad (4.5)$$

A homogeneous Dirichlet data is imposed on the outflow boundary on the right side of the domain

$(10^{-3}, 10^{-2})$	$(0, 10^{-2})$
$(10^{-4}, 10^{-2})$	$(10^{-2}, 10^{-3})$

FIG. 6. Values of D_{11} and D_{22} on domain $[0, 1] \times [0, 1]$.

$$g^o(y) \equiv 0, \quad \forall t \in [0, T]. \quad (4.6)$$

Both the top and the bottom sides are noflow boundaries. The initial condition is given as $u_0(x, y) \equiv 0$. Because the analytical solution is not available, we compare the numerical solutions generated by the nonoverlapping DDM with the ELLAM solution on the entire domain. The numerical solutions obtained with 10 time steps are presented in Fig. 7 and Table II. The tolerance for both the inner CG iterations and the outer PCG iterations are chosen to be 10^{-6} . These results show that the characteristic nonoverlapping DDM generates comparable solutions with the ELLAM scheme without a DDM even though the diffusion term has jumps.

To observe the convergence rate of the additive Schwarz characteristic nonoverlapping DDM preconditioner, we measure the number of outer PCG iterations for the preconditioner and the number of iterations for the ELLAM scheme without DDM in Table III for each of the 10 time steps. On the basis of the related theoretical convergence analysis for overlapping or nonoverlapping additive Schwarz DDM preconditioners for elliptic or non self-adjoint parabolic PDEs [1–4, 17], we expect that the convergence rate of the additive Schwarz characteristic nonoverlapping DDM preconditioner is of the form $(H/h)^2$ up to some $\ln(H/h)$ factors for any fixed time steps. Here H is the diameter of coarse mesh. Our preliminary numerical results in Table III confirmed this convergence behavior.

V. SUMMARY

This article is a continuation of the efforts in [21, 22, 23]. We base on an ELLAM formulation and an abstract additive Schwarz framework to develop a quasi-two-level, coarse-mesh-free, characteristic nonoverlapping domain decomposition method for the solution of time-dependent convection-diffusion transport PDEs in multiple space dimensions. This method fully utilizes the hyperbolic nature of governing convection-diffusion PDEs to choose the appropriate artificial boundary conditions and interface matching conditions across the internal boundaries of different subdomains. Numerical results show that the developed domain decomposition method generates accurate numerical solutions

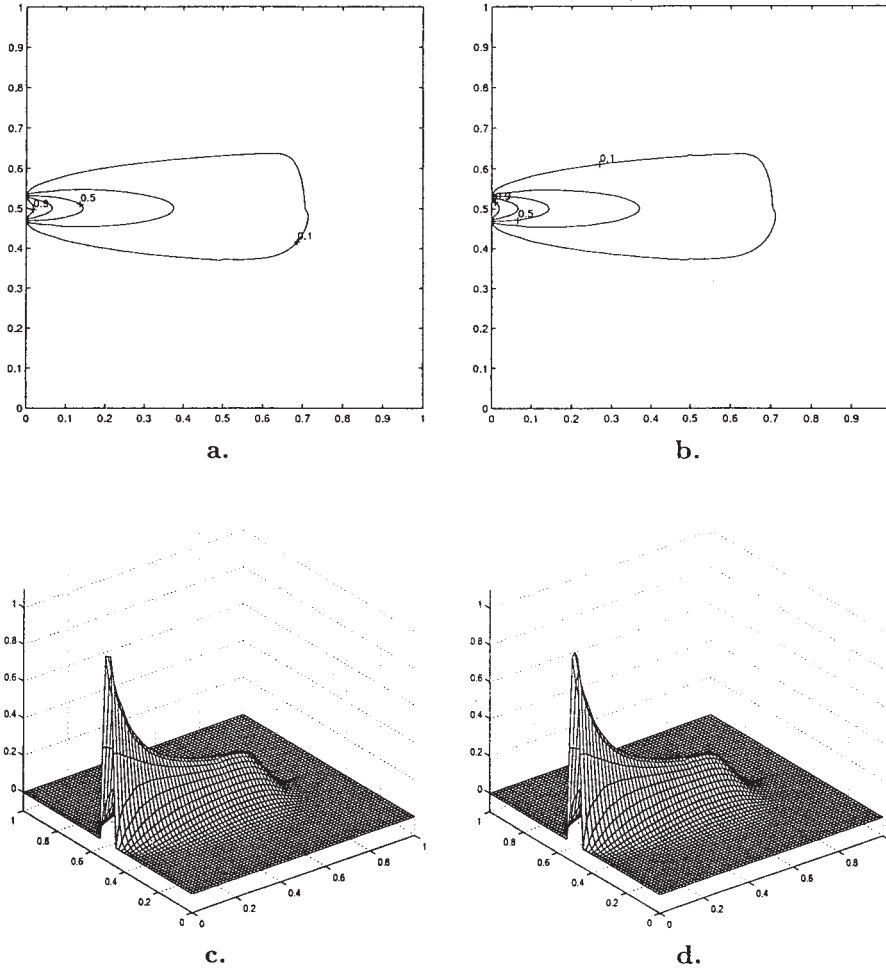


FIG. 7. Contour and surface plots of horizontal flow with $h = 1/128$. (a) No decomposition; (b) 2×2 decomposition; (c) no decomposition; (d) 2×2 decomposition.

without noticeable artifacts. Theoretical analysis of the proposed domain decomposition method will be presented in our future work.

The authors express their sincere thanks to the referees for their very valuable comments and suggestions, which greatly improved the quality of this article.

TABLE II. Approximation errors for the horizontal flow.

	No decomposition		Decomposition	
h	1/128	1/256	1/128	1/256
No. of subdomains	N/A	N/A	2×2	2×2
U_{\min}	0	0	0	0
U_{\max}	1.017, 343	1.010, 969	1.036, 412	1.010, 981

TABLE III. Numbers of iterations for the horizontal flow with $h = 1/128$.

	No. of iterations at 10 time steps									
No decomposition	93	92	92	94	95	93	92	92	92	92
2×2 decomposition	20	19	23	22	23	22	19	22	23	23

References

1. B. F. Smith, P. E. Bjørstad, and W. D. Gropp, Domain decomposition, Cambridge University Press, 1996.
2. J. Xu and J. Zou, Some nonoverlapping domain decomposition methods, *SIAM Rev* 40 (1998), 857–914.
3. X. C. Cai, Additive Schwarz algorithms for parabolic convection-diffusion equations, *Numer Math* 60 (1991), 41–61.
4. X. C. Cai, Multiplicative Schwarz methods for parabolic problems, *SIAM J Sci Comput* 15 (1994), 587–603.
5. M. Ciccoli, Adaptive domain decomposition algorithms and finite volume/finite element approximation for advection-diffusion equations, *J Sci Comput* 11 (1996), 299–341.
6. F. Gastaldi, L. Gastaldi, and A. Quarteroni, Adaptive domain decomposition methods for advection dominated equations, *East-West J Numer Math* 4 (1996), 165–206.
7. R. Rannacher and G. Zhou, Analysis of a domain-splitting method for nonstationary convection-diffusion problems, *East-West J Numer Math* 2 (1994), 151–172.
8. H. Wang, R. E. Ewing, G. Qin, S. L. Lyons, M. Al-Lawatia, and S. Man, A family of Eulerian-Lagrangian localized adjoint methods for multidimensional advection-reaction equations, *J Comput Phys* 152 (1999), 120–163.
9. J. Douglas, Jr. and T. F. Russell, Numerical methods for convection-dominated diffusion problems based on combining the method of characteristics with finite element or finite difference procedures, *SIAM J Numer Anal* 19 (1982), 871–885.
10. O. Pir, On the transport-diffusion algorithm and its application to the Navier-Stokes equations, *Numer Math* 38 (1982), 309–332.
11. X. Tai, T. Johansen, H. Dahle, and M. Espedal, A characteristic domain splitting method, Glowinski et al., editors, *Domain decomposition methods in science and engineering*, Proceedings of 8th International Conference on Domain Decomposition Methods, John Wiley, New York, 1997, pp 317–323.
12. M. A. Celia, T. F. Russell, I. Herrera, and R. E. Ewing, An Eulerian-Lagrangian localized adjoint method for the advection-diffusion equation, *Adv Water Resour* 13 (1990), 187–206.
13. T. F. Russell and M. A. Celia, An overview of research on Eulerian-Lagrangian localized adjoint methods (ELLAM), *Adv Water Resour* 25 (2002), 1215–1231.
14. H. Wang, H. K. Dahle, R. E. Ewing, M. S. Espedal, R. C. Sharpley, and S. Man, An ELLAM scheme for advection-diffusion equations in two dimensions, *SIAM J Sci Comput* 20 (1999), 2160–2194.
15. M. Al-Lawatia, R. C. Sharpley, and H. Wang, Second-order characteristic methods for advection-diffusion equations and comparison to other schemes, *Adv Water Resour* 22 (1999), 741–768.
16. H. Wang, M. Al-Lawatia, and S. A. Telyakovskiy, Runge-Kutta characteristic methods for first-order linear hyperbolic equations, *Numer Meth PDEs* 13 (1997), 617–661.
17. S. C. Brenner and L. R. Scott, *Mathematical theory of finite element methods*, Springer, Berlin, 2002.
18. H. Wang, R. Ewing, and T. Russel, Eulerian-Lagrangian localized adjoint methods for convection-diffusion equations and their convergence analysis, *IMA J Numer Anal* 15 (1995), 405–459.

19. H. Wang, An optimal-order error estimate for an ELLAM scheme for two-dimensional linear advection-diffusion equations, *SIAM J Numer Anal* 37 (2000), 1338–1368.
20. B. A. Finlayson, *Numerical methods for problems with moving fronts*, Ravenna Park Publishing, Seattle, 1992.
21. H. Wang and M. Al-Lawatia, An Eulerian-Lagrangian substructuring domain decomposition method for unsteady-state advection-diffusion equations, *Numer Meth PDEs* 17 (2001), 565–583.
22. H. Wang, M. Al-Lawatia, and R. C. Sharpley, A characteristic domain decomposition and space-time local refinement method for first-order linear hyperbolic equations with interfaces, *Numer Meth PDEs* 15 (1999), 1–28.
23. H. Wang, H. K. Dahle, R. E. Ewing, T. Lin, and J. E. Våg, ELLAM-based domain decomposition and local refinement methods for advection-diffusion equations with interfaces, Keyes and Xu, editors, *Contemporary Mathematics*, Vol. 180, American Mathematical Society, 1994, pp 361–366.